Effects of the nonlinear stage of Jeans instability on the pairwise correlation function

A. V. Gurevich, M. I. Zel'nikov, and K. P. Zybin

I. E. Tamm Theoretical Department, P. N. Lebedev Physics Institute, Russian Academy of Sciences, 117924 Moscow, Russia

(Submitted 8 November 1994)
Zh. Éksp. Teor. Fiz. **107**, 1377–1392 (May 1995)

We have developed a statistical method to describe the strongly nonlinear stage in the evolution of large-scale structure in the universe. The method is based on the theory of nonlinear contraction of dark matter at an isolated density peak[1–3] and a scheme for the successive gravitational capture of smaller objects by larger ones. We have devised a diagrammatic technique that enables one, in principle, to calculate steady-state correlation functions of any order. We have derived an analytic expression for the pairwise correlation function ξ in the strong-correlation range $\xi \gg 1$, and we have shown that it is fully consistent with the well known observed behavior $\xi \propto r^{-\alpha}, \alpha \approx 1.8$. In this expression, α is a scaling parameter that characterizes the three-dimensional contraction of self-entrained nondissipative matter. © *1995 American Institute of Physics.*

1. INTRODUCTION. PHYSICAL PICTURE OF THE EMERGENCE OF STRUCTURE IN THE DISTRIBUTION OF MATTER IN THE UNIVERSE

The existence of large-scale structure—galaxies, clusters of galaxies, superclusters—derives from the Jeans instability of small perturbations that arise in the early universe. Establishing the link between the properties of the original irregularities and the observed distribution of large-scale objects is one of the most important problems in theoretical cosmology. The problem is an extremely difficult one and is still far from being solved, despite the best efforts of theoreticians. The principal difficulties have to do with the nonlinear and nonstationary way in which instability develops. Normally, this problem is approached via numerical modeling.[4,5] In the present paper, we solve it using statistical methods based on previously obtained analytic dynamical equations.

Our current understanding is that most of the mass in the universe consists of dark matter, a conclusion drawn from the rotation curves of galaxies, the distribution of hot gas, and the motion of galaxies within clusters.[6] Unfortunately, we do not know what particles comprise that dark matter, but we can state with some confidence that they are cold (nonrelativistic) and matter-dominated, and that they interact with baryon matter and with one another very weakly.

It is commonly assumed that the early universe contained small nonthermal perturbations in the distribution of dark matter, and that they emerged from quantum fluctuations at the time of inflation.[7] When the expansion dynamics of the universe began to be dominated by dark matter, the perturbations acquired something like a Zel'dovich–Harrison spectrum $P(k) \propto k$ at long wavelengths. At short wavelengths, the perturbation spectrum rises monotonically with increasing wave number k, peaks, and then rapidly declines. The actual location of the maximum, $k = k_{\max}$, depends on the mass of the particles that make up the dark matter. The existence of a maximum and the rapid falloff of the spectrum as $k \to \infty$ are important consequences of the linear dynamics of perturbations in the early universe at time $t = t_i$ when particles of dark matter are falling out of thermal equilibrium ("hardening").

The linear theory of the development of small inhomogeneities after "hardening" is well known.[8] Here we indicate those properties of the linear solution that we will subsequently take advantage of. In general, perturbations are specified by four scalar functions,

$$\delta(\mathbf{x},t) \equiv \frac{\rho(\mathbf{x},t)-\rho_0(t)}{\rho_0(t)}, \quad \mathbf{u}(\mathbf{x},t),$$

where δ is the density inhomogeneity, ρ_0 is the background density, and $\mathbf{u}$ is the peculiar velocity of the matter.

In an expanding universe, the equations for the evolution of perturbations have two linearly independent solutions, one growing and the other damped. With the passage of time, then, one growing solution begins to dominate among the density perturbations:

$$\delta(\mathbf{x},t) = \left\{ \delta(\mathbf{x},t_i)\dot{D}_2(t_i) + \frac{\nabla \mathbf{u}(t_i)}{a(t_i)} D_2(t_i) \right\} D_1(t) E^{-1}, \qquad (1)$$

where $a(t)$ is a scale factor and $E = D_1(t_i)\dot{D}_2(t_i) - D_2(t_i)\dot{D}_1(t_i)$. The functions $D_1(t)$ and $D_2(t)$ are the growing and decaying solutions of the equation

$$\ddot{D} + 2\frac{\dot{a}}{a}\dot{D} = \rho_0(t) D. \qquad (2)$$

Dots in Eqs. (1) and (2) denote differentiation with respect to time. We see that by the end of the linear stage we have pure potential motion that can be specified by just one scalar function instead of four,

$$\tilde{\delta}(\mathbf{x},t_i) = \delta(\mathbf{x},t_i) + \frac{\nabla \mathbf{u}(t_i)}{a(t_i)} \frac{D_2(t_i)}{\dot{D}_2(t_i)}, \qquad (3)$$

which we will refer to as the effective density. In other words, we obtain exactly the same picture of how gravitational instability develops in the linear stage at late times whether we take the initial distribution $\delta(\mathbf{x},t_i)$ of density irregularities to be equal to the effective density (3) or we

 1063-7761/95/050769-08$10.00

assume an initial velocity $\mathbf{u}(\mathbf{x},t_i)=\mathbf{0}$. From here on, we take the density perturbation δ to mean the effective density $\tilde{\delta}$. Note that one could introduce yet another scalar function to specify the growth of perturbations in lieu of the effective density $\tilde{\delta}$, for example the potential ψ of the gravitational field.

We emphasize an important property of the growing solution (1): perturbation amplitudes grow with time in a scale-invariant manner. This implies that nonlinear effects will tend to make themselves felt in the vicinity of the maxima of the initial distribution $\tilde{\delta}$. In Refs. 1–3, the present authors reported on an investigation of the nonlinear dynamics of dark matter in the neighborhood of an isolated maximum of $\tilde{\delta}$. Here we detail the principal analytical results.

Near a density maximum, the development of a potential flow leads, in some finite time, to the emergence of a singularity at which the density goes to infinity. This is followed by the development of a multistream flow as a result of gravitational self-entrainment of matter, with the number of streams increasing with time. This mixing in the vicinity of the initial maximum eventually produces a nondissipative gravitational singularity—a steady-state, self-entrained, spherically symmetric distribution of matter with a central singularity of the form

$$\rho(r)=\tilde{\rho}\left(\frac{r}{R}\right)^{-a}. \tag{4}$$

Here α varies over the range 1.7–1.9, and we will adopt the mean value $\alpha\approx 1.8$. We see that in the steady state, α does in fact take on a constant value, irrespective of the shape and scale of the initial maximum. This is a manifestation of the fundamental scaling property of the three-dimensional nonlinear gravitational contraction of cold nondissipative matter. Any nondissipative gravitational singularity, then, will be a spherically symmetric structure, with a density distribution (4) specified by just the two parameters R and $\tilde{\rho}$. The radius R is the comoving size of the density maximum at time t_R, where $\tilde{\delta}(\mathbf{0},t_R)=\delta_0\sim 1$; t_R is the characteristic time at which nonlinear separation of the peak from the general cosmological expansion takes place, at which point the peak's physical (proper) size is fixed. We denote the corresponding redshift by z_R. From the definition of t_R, at $t>t_R$ the peak will already have passed through the nonlinear stage of evolution and turned into a nondissipative gravitational singularity of size R. Subsequently, it behaves like an isolated object of constant physical size with a time-independent internal density distribution. The relationship between the object's size R' in comoving coordinates at the present time and its comoving size R at the time of formation is

$$R'=R/(1+z_R). \tag{5}$$

In the present paper, the object in question is assumed to be a gravitationally bound collection of *dark* matter with density distribution (4) and size R. Luminous matter constitutes only a small fraction by mass compared with dark matter; it emits radiation, by virtue of its dissipative nature, losing energy and descending to the bottom of a potential well produced by the dark matter. Observable luminous objects thus identify the central regions of a nondissipative gravitational singularity. The luminous component exercises a minor influence (which we ignore here) on the overall dynamics of matter during the time the object takes shape.

As we showed above, the initial spectrum $P(k)$ of irregularities grows with increasing k, peaks, and then declines. That being the case, objects whose dimensions correspond to the spectral peak are formed first, to be followed by others that are larger and larger. As they form, large-scale objects can capture smaller objects gravitationally, and thus a hierarchical structure can develop with time.

One important quantity that characterizes the degree to which smaller objects in a hierarchical structure are embedded within larger ones is the filling parameter $\epsilon(R)$, i.e., the probability that an object of size R is enclosed by a larger one. It depends on the size dependence of the number density $n(R)$ of peaks in the initial density distribution, and on their spatial correlations. If the spectrum is a power law at long wavelengths, $P(k)\propto k^n$, then for large enough R, scale invariance dictates that

$$n(R)dR=3\beta R^{-4}dR, \tag{6}$$

where β is a dimensionless parameter that depends on the spectral index n. The concentration of objects larger than R is then $n(>R)=\beta(R^{-3}-R_f^{-3})$, where R_f is the size of the largest objects formed up to the present. Neglecting positional correlations among the objects, we can estimate the filling parameter to be

$$\epsilon(R)=\int_R^{R_f}\frac{4}{3}\pi R^3 n(R)dR=4\pi\beta\ \ln\frac{R_f}{R}. \tag{7}$$

Evaluating β based on observations of clusters and groups of galaxies,[9] we have

$$\beta\approx 6.4\cdot 10^{-3}.$$

(This figure may be somewhat low if the assumed contribution of dark matter to the total mass has been underestimated.) Given a power law with spectral index n, the theoretical upper limit on β is also small[10]:

$$\beta<0.016\left(\frac{6}{n+5}\right)^{3/2}.$$

We thus see that the degree of object embedding in an actual hierarchical structure is not very large. The hierarchical picture discussed above is based on the theory of the self-consistent mean field, which is rigorously valid only prior to the formation of primordial objects. Once the latter have formed, additional fluctuations arise as a product of the clumping of the initially smooth medium. Upon subsequent evolution, objects start to collide with one another, whereupon Eq. (4) for the density distribution begins to change with time. It can be shown, however, that the time τ_c in which the shape of the distribution can change substantially is much greater than the Jeans time.

The observed quasistationary hierarchical picture of the large-scale distribution of matter in the universe is thus bounded in both space and time. Indeed, on scales $R>50$–100 Mpc, perturbations are in the linear growth regime: nonlinear contraction and kinetic mixing have not yet occurred.

On scales $R \approx 10$–50 Mpc, inhomogeneities are in a nonsteady nonlinear regime in which the first singularities, caustics, and partially mixed objects come into being. On scales $R < 10$ Mpc, we have essentially steady-state structures, and for R not too small, their ages are $t < \tau_c$, so those structures have yet to undergo collisional relaxation. It is precisely on scales $R < 10$ Mpc that the theory discussed here is applicable, and we limit our subsequent discussion largely to such scales.

This paper is organized as follows. The model used to calculate the correlations is described in Sec. 2. Section 3 describes the calculation of j-point correlation functions, and we establish the relationship between the initial positional correlations among the objects that have been formed, prior to gravitational capture, and the final correlations after the linear stage of Jean instability. We develop a diagrammatic technique that enables one to express the final correlation functions as sums of simpler diagrams. We indicate which diagrams might be major contributors when the filling factor $\epsilon(R)$ is small. Finally, making a number of simplifying assumptions, we calculate the pairwise correlation function in Sec. 4, and we conclude in Sec. 5 with a summary of the principal results. We show that in the strong-correlation regime $\xi \gg 1$, the dependence of the correlation function on the separation r between objects is governed exclusively by nonlinear contraction laws. This behavior is universal in nature, and is completely consistent with the observational data. We also discuss the dependence of the magnitude of the pairwise correlation function on the number density of the objects under consideration (or on the mean separation between them).

2. MODELING THE ONSET OF CORRELATIONS

Our overall objective here is to find the distribution of objects that have gone through a nonlinear stage in a region that has come to a steady state. Underlying the method that we employ to describe the strongly nonlinear stage in the evolution of structure in the universe, we have, first, the theory devised in Refs. 1–3 for the nonlinear contraction of nondissipative cold matter in an isolated density peak, and second, a scheme for the systematic capture of smaller objects by larger ones.

To implement this description, we examine the N-point statistics of the spatial locations of all objects of all possible sizes that have been formed. The starting point in our theory is the joint probability distribution $P(\mathbf{y}_i, R_i)$ for the formation of N objects with given sizes R_i centered at the given points $\mathbf{y}_i$.

The influence of nonlinear dynamics on the statistical properties of a system of objects is usually described by an infinite hierarchy of coupled equations for the moments of the N-particle distribution functions (BBGKY hierarchy). In the case of self-gravitating matter, this problem has been widely discussed in the literature, notably in Peebles' book.[11] The set of coupled equations is usually solved by cutting off the sequence and neglecting higher-order moments. As indicated above, however, a strongly correlated singular distribution of matter arises in the vicinity of maxima of the effective density, where the pairwise correlation function $\xi \gg 1$ (this holds for higher moments as well). As a result, the cutoff approach is ill-advised under these circumstances. The formation of strongly correlated distributions will yield only to a well-founded approach such as the one underlying our method. To describe the emergence of these distributions, we make use of the transition probability derived from the nonlinear equation (4). This enables one to find the relationship between the initial and final values of the correlation functions directly, and comprises the most novel aspect of our method. It makes it possible to avoid solving a set of coupled equations, while effectively allowing for the entire BBGKY hierarchy at $\xi \gg 1$.

As noted above, after the effective density (3) reaches $\delta \sim 1$ at one of its maxima, a nondissipative gravitational singularity will form fairly rapidly. We will assume in our statistical model that this occurs instantaneously. If some large object is captured by a given singularity, we assume that the probability $f(r)$ of finding it in some unit volume at distance r from the center of the singularity at the present time is proportional to the density (4) of matter:

$$f(r,R) = \frac{3-\alpha}{4\pi} R'^{-3} \theta(R'-r) \left(\frac{r}{R'}\right)^{-\alpha}. \tag{8}$$

The constant in Eq. (16) can be determined by requiring that the mass contained within the volume $r < R$ be conserved as the nondissipative gravitational singularity forms. Here R' is the comoving size of the object at the present time, and is given by Eq. (5).

The density distribution within a nondissipative gravitational singularity, as governed by the nonlinear contraction laws, of course only take the form (4) asymptotically as $r \to 0$, and yield an error of order 1 at $r \sim R'$. One should therefore anticipate sizable corrections to the probability distribution (8) at distances $r \geqslant R'$.

We now determine the conditions under which one object is captured by another. An object of size R_2 centered at the point $\mathbf{y}_2$ will capture another object of size R_1 located at $\mathbf{y}_1$ if

$$R_1 < R_2 \quad \text{and} \quad |\mathbf{y}_1 - \mathbf{y}_2| < R_2. \tag{9}$$

If (9) fails to hold for any object $(\mathbf{y}_2, R_2)$, we assume that the object $(\mathbf{y}_1, R_1)$ remains in place.

In calculating diagrams of higher order in the number of participating objects, the distribution of objects of a given size with respect to their epoch of formation (redshift) is important. Strictly speaking, there is a large dispersion in the times of formation, but in this paper we make the simplifying assumption that all objects of a given size R form simultaneously at redshift z_R. We choose for z_R that time at which the majority of objects of size R form. The actual value of z_R is governed by the initial spectrum of inhomogeneities $P(k, t_i)$. Assuming that the Fourier components

$$\delta_{\mathbf{k}}(t) = \int_{-\infty}^{+\infty} e^{-i\mathbf{k}\mathbf{x}} \delta(\mathbf{x}, t) d\mathbf{x} \tag{10}$$

have random phases, we have for the spectrum

$$\langle \delta_{\mathbf{k}}(t) \delta_{\mathbf{k}'}(t) \rangle = (2\pi)^3 P(k,t) \delta(\mathbf{k} + \mathbf{k}'). \tag{11}$$

To describe the formation process for objects of size R, we make use of a density distribution smoothed on a scale R, with a normalized smoothing function $w(s)$ that falls off rapidly at infinity:

$$\int_{-\infty}^{+\infty} w(s)\, d\mathbf{s}=1.$$

The smoothed density function $\delta(\mathbf{x},R,t)$ can then be written in the form

$$\hat{\delta}(\mathbf{x},R,t)=\int_{-\infty}^{+\infty} w\left(\frac{|\mathbf{x}-\mathbf{y}|}{R}\right)R^{-3}\delta(\mathbf{y},t)d\mathbf{y}=1. \qquad (12)$$

As mentioned above, the nonlinear contraction stage at an individual peak begins at a time t given by $\delta(\mathbf{x},t_0)\sim 1$. Most objects of size R are formed when

$$\langle\delta^2(\mathbf{x},R,t)\rangle=\delta_0\sim 1. \qquad (13)$$

Now δ_0 is not known accurately, but for a power-law spectrum, it obviously depends on the smoothing scale R, and is a universal constant. The growth of inhomogeneities is governed by Eq. (1); at the matter-dominated stage,

$$D_1(t)=D_1(t_i)(1+z(t_i))/(1+z(t)). \qquad (14)$$

For initial perturbations with a power-law spectrum

$$P(k,t_i)=Pk^n,$$

and using (10)–(14), we easily obtain an expression for z_R:

$$1+z_R=\left(\frac{R_f}{R}\right)^{(n+3)/2},$$
$$R_f=[C_w\delta_0^{-1}P^{1/2}]^{2/(n+3)}, \qquad (15)$$

where C_w is a constant of order 1.

Equations (5) and (15) yield a relation between the comoving size of an object at the present time and at birth:

$$R'=\frac{R}{1+z_R}=R^{(n+5)/2}R_f^{-(n+3)/2}. \qquad (16)$$

We make use of this relation below.

To summarize, every object in our model can be characterized by its coordinates $\mathbf{x}_i$ and size R_i. The structure of the distribution of matter can be described by a statistically large number N of points in physical space $\mathbf{x}$ and dimension space R. Nonlinear evolution is completely described by the random sequential capture of small objects by large ones. The rule for the transition probability corresponding to a single capture event is given by Eqs. (8) and (9). To calculate the final j-point correlation functions, we also need to know the initial correlations of all N objects and the rules for calculating the transition probabilities of multiple captures. These questions are discussed in the next section.

3. CALCULATION OF j-POINT CORRELATION FUNCTIONS

Let us calculate the transition probability for a test particle that has been trapped by *several* other objects. Let the first capturing particle have a radius R_1. An object of size $R_2>R_1$ is then formed, capturing the first object. The probability $W(\mathbf{r})$ of a transition of the test particle to a final state given by the vector $\mathbf{r}$ relative to the center of the second object can be put in the form

$$W(\mathbf{r})=\int f(|\mathbf{r}+\mathbf{x}|,R_1)f(|\mathbf{x},R_2|)d\mathbf{x},$$

if, as we assume, neither collisions nor tidal forces manage to alter the internal structure of the captured object. We stipulate from here on that any such quantity—the probability density for finding objects in unit volume (per unit size interval) in the vicinity of the given points—will for brevity simply be called the object detection probability density at those points (for objects of a certain size).

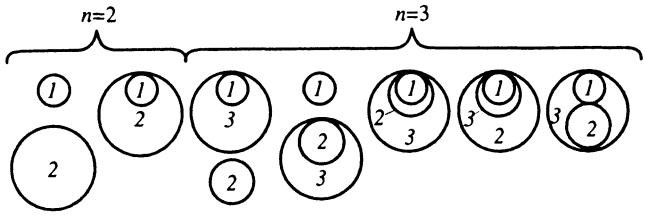

FIG. 1. Sketch of all possible ways to spatially superimpose $n\leq 3$ objects on one another, as required in the sum (17) for $j=2$.

Since the various trapped objects rapidly "forget" their initial correlations as they are mixed, we can independently calculate the conditional transition probability density for several objects incorporated into a larger one, and multiply them together. For example, if two objects of size R_1 and R_2 are captured by an object of size R_3 located at $\mathbf{x}_3$, the probability density for detecting them after mixing at $\mathbf{x}_1$ and $\mathbf{x}_2$ will simply be

$$W(\mathbf{x}_1,\mathbf{x}_2)=f(|\mathbf{x}_1-\mathbf{x}_3|,R_3)f(|\mathbf{x}_2-\mathbf{x}_3|,R_3).$$

Similarly, we can calculate the transition probability density in the general case. Let the probability density for finding n objects of size R_i at the points $\mathbf{x}_i$ be $W_a^n(\mathbf{x}_i,\mathbf{y}_i,R_i)$, given that they were formed at the points $\mathbf{y}_i$. Then the probability density for finding j objects with sizes $R_1,\ldots,R_j$ at the present time at the points $\mathbf{x}_1,\ldots,\mathbf{x}_j$ can be put in the form

$$P(\mathbf{x}_1,\ldots,\mathbf{x}_j,R_1,\ldots,R_j)=\sum_a P_a(\mathbf{x}_1,\ldots,\mathbf{x}_j,R_1,\ldots,R_j)$$
$$=\sum_{n=j}^{\infty}\sum_a\int\ldots\int W_a^n(\mathbf{x}_i,\mathbf{y}_i,R_i)P_a^n$$
$$\times(\mathbf{y}_i,R_i)\prod_{n=1}^{n}d\mathbf{y}_i\prod_{i=j+1}^{n}d\mathbf{x}_i dR_i. \qquad (17)$$

Here the subscript a specifies the various ways in which n objects can be superimposed upon one another (in other words, the various capture configurations). For example, Fig. 1 represents all possible superimposition schemes for objects 1, 2, and 3 with $j=2$, $n=2,3$.

Note that when the capture configurations are enumerated via (17), only those objects that actually capture at least one of the smaller objects 1,...,j are to be taken into consideration; objects that are themselves captured but that capture no others are not.

Finally, we note that the summation from n to ∞ in (17) only makes sense if arbitrarily large objects exist in the universe. More realistically, given that galaxies have evolved for only a finite time, for example, $n<(2-3)j$ is a sufficient condition—all the more so as terms with large n must be small, reflecting the smallness of the filling factor ϵ.

In Eq. (17), $P_a^n(\mathbf{y}_i,R_i)$ is the probability density for producing a given set of n objects at points $\mathbf{y}_i$ in a configuration a such that no other external objects capture any of them. We have

$$P_a^n(\mathbf{y}_i,R_i)=\Theta_a^n(\mathbf{y}_i,R_i)P^n(\mathbf{y}_i,R_i),$$

where $P^n(\mathbf{y}_i,R_i)$ is the probability density for producing some particular n objects with sizes R_i at points $\mathbf{y}_i$, while others fall where they may, so long as they are not captured. $\Theta_a^n(\mathbf{y}_i,R_i)$ is an indicator function that equals 1 if the objects are in configuration a and 0 otherwise. These test the conditions (9) for any pair of objects. For example, with $j=2$, $n=2,3$, for the configurations specified above,

$$\Theta_0^2=\theta(|\mathbf{y}_1-\mathbf{y}_2|-R_2),$$

$$\Theta_1^2=\theta(R_2-|\mathbf{y}_1-\mathbf{y}_2|),$$

$$\Theta_2^3=\theta(R_3-R_2)\theta(R_3-|\mathbf{y}_1-\mathbf{y}_3|)\theta(|\mathbf{y}_2-\mathbf{y}_3|-R_3)\times\theta(|\mathbf{y}_i-\mathbf{y}_2|-R_2)+\theta(R_3-R_1)\theta(R_2-R_3)\times\theta(R_3-|\mathbf{y}_1-\mathbf{y}_3|)\theta(|\mathbf{y}_2-\mathbf{y}_3|-R_2),$$

$$\Theta_3^3=\theta(R_3-R_2)\theta(R_3-|\mathbf{y}_2-\mathbf{y}_3|)\theta(|\mathbf{y}_1-\mathbf{y}_3|-R_3)\times\theta(|\mathbf{y}_1-\mathbf{y}_2|-R_2),$$

$$\Theta_4^3=\theta(R_3-R_2)\theta(R_3-|\mathbf{y}_2-\mathbf{y}_3|)\theta(R_2-|\mathbf{y}_1-\mathbf{y}_2|),$$

$$\Theta_5^3=\theta(R_2-R_3)\theta(R_3-R_1)\theta(R_3-|\mathbf{y}_1-\mathbf{y}_3|)\times\theta(R_2-|\mathbf{y}_2-\mathbf{y}_3|),$$

$$\Theta_6^3=\theta(R_3-R_2)\theta(R_3-|\mathbf{y}_2-\mathbf{y}_3|)\theta(R_3-|\mathbf{y}_1-\mathbf{y}_3|)\times\theta(|\mathbf{y}_1-\mathbf{y}_2|-R_2).$$

The corresponding transition probability densities take the form

$$W_0^2=\delta(\mathbf{x}_1-\mathbf{y}_1)\delta(\mathbf{x}_2-\mathbf{y}_2),$$

$$W_1^2=f(|\mathbf{x}_1-\mathbf{x}_2|,R_2)\delta(\mathbf{x}_2-\mathbf{y}_2)$$

$$W_2^3=f(|\mathbf{x}_1-\mathbf{x}_3|,R_3)\delta(\mathbf{x}_2-\mathbf{y}_2)\delta(\mathbf{x}_3-\mathbf{y}_3),$$

$$W_3^3=f(|\mathbf{x}_2-\mathbf{x}_3|,R_3)\delta(\mathbf{x}_1-\mathbf{y}_1)\delta(\mathbf{x}_3-\mathbf{y}_3),$$

$$W_4^3=f(|\mathbf{x}_1-\mathbf{x}_2|,R_2)f(|\mathbf{x}_2-\mathbf{x}_3|,R_3)\delta(\mathbf{x}_3-\mathbf{y}_3),$$

$$W_5^3=f(|\mathbf{x}_1-\mathbf{x}_3|,R_3)f(|\mathbf{x}_2-\mathbf{x}_3|,R_2)\delta(\mathbf{x}_2-\mathbf{y}_2),$$

$$W_6^3=f(|\mathbf{x}_1-\mathbf{x}_3|,R_3)f(|\mathbf{x}_2-\mathbf{x}_3|,R_3)\delta(\mathbf{x}_3-\mathbf{y}_3).$$

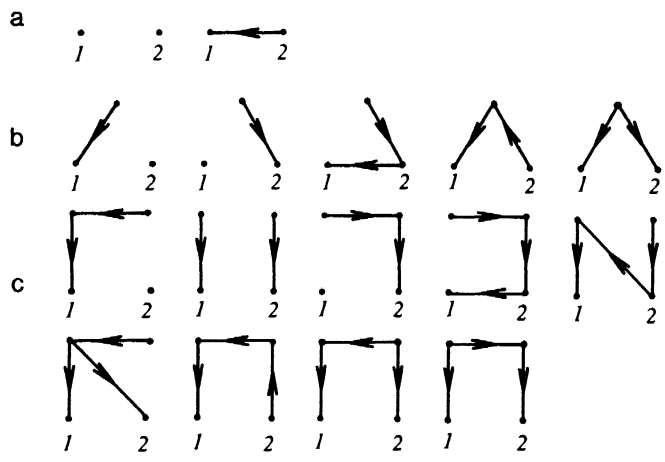

FIG. 2. All capture configurations that contribute to the pairwise ($j=2$) correlation function for a) $n=2$, b) $n=3$, and c) $n=4$ participating objects.

Every term in the sum (17) can be put into correspondence with a diagram according to the following rules:

1) Every arrow $i\vec{k}$ corresponds to a factor $f(|\mathbf{x}_i-\mathbf{x}_k|,R_i)$.
2) A vertex with $i\neq 1,...,j$ at which no arrows terminate, $i\rightarrow$, corresponds to a factor $\delta(\mathbf{x}_i-\mathbf{y}_i)$.
3) An additional factor $P_a^n(\mathbf{y}_i,R_i)$ corresponds to an entire diagram with n vertices.
   Integration is carried out over all $\mathbf{x}_i$, $\mathbf{y}_i$, and R_i except for $\mathbf{x}_1,...,\mathbf{x}_j$ and $\mathbf{R}_1,...,\mathbf{R}_j$. The sum (17) spans all possible diagrams containing $n\geqslant j$ vertices for which
4) no more than one arrow terminates at each vertex;
5) the only vertices from which no arrows originate are 1,...,j.

In this way, the only diagrams that contribute to the sum are those that contain no loops or parts not linked to vertices 1,...,j. All feasible diagrams with $n\leqslant 4$ that contribute to the two-point correlation function ($j=2$) are shown in Fig. 2.

By summing all possible diagrams for a given j, we obtain the probability density for finding j objects of a given size at a given location at the present time. Thus, in principle, Eq. (17) and the diagrammatic technique just described enable one to calculate the final j-point correlation function when one knows the probability density $P^n(\mathbf{y}_i,R_i)$ at formation time for any initial arrangement of an arbitrary number n of uncaptured objects.

The quantity $P^n(\mathbf{y}_i,R_i)$ specifies the probability of a given disposition of density maxima of various sizes in the linear stage, and as we have suggested, it is completely predetermined by the initial spectrum of inhomogeneities $P(k,t_i)$. Calculating this quantity for an arbitrary spectrum is a separate nontrivial problem that we have yet to solve. Therefore, here we merely adopt an estimate of $P^n(\mathbf{y}_i,R_i)$ in a certain simple case: we consider a situation in which the positions of all objects formed are uncorrelated. This simplification can be shown not to alter the form of the pairwise correlation function ξ in the strong-correlation range $\xi\gg 1$. Assuming then that the total number of objects formed is large, we obtain

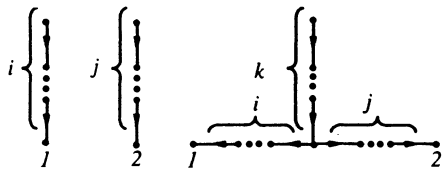

FIG. 3. Overview of all diagrams that contribute to the pairwise correlation function for $i,j,k=0,1,2,\ldots$.

$$P^n(\mathbf{y}_1,R_i)=n(R_1)\ldots n(R_n)\left\{1-\epsilon(v)+\frac{1}{2}\epsilon^2(v)+O(\epsilon^3)\right\}, \tag{18}$$

where

$$\epsilon(v)=\int_{v(\mathbf{y}_i,R_i)} n(R)dRd\mathbf{y}.$$

The domain of integration here is the entire region v of $(\mathbf{y},R)$ space containing objects that have trapped at least one of the objects $(\mathbf{y}_i,R_i)$. The number density of objects with size between R and $R+dR$ is $n(R)\,dR$, and is given by Eq. (6) for a scale-invariant spectrum.

4. PAIRWISE CORRELATION FUNCTION

We now consider the observationally more interesting pairwise correlation function in more detail; it can be calculated using Eq. (17) with $j=2$. We employ (18) to estimate P^n. For the case of interest here, with small n, note that $\epsilon(v)$ is a small parameter proportional to the filling factor (7):

$$\epsilon(v)\leqslant\sum_{i=1}^{n}\int_{R_i}^{R_f}\frac{4}{3}\pi R^3 n(R)dR=4\pi\beta\sum_{i=1}^{n}\ln\frac{R_f}{R_i}.$$

All of the diagrams that contribute to the pairwise correlation function consist of one or two linked segments, and take the form illustrated in Fig. 3.

It can easily be shown that any of these diagrams that contain a "tail" made up of k branches (or two tails with k branches *in toto*) introduce a small correction of order ϵ^k to the corresponding tailless diagram. Thus, none of the leading terms in the expansion in ϵ have tails. Starting with the leading term, we can label these diagrams using the small parameter ϵ as shown in Fig. 4.

By virtue of the uniformity and isotropy of the statistics of the initial perturbations, the desired probability density and the pairwise correlation function depend solely on $r=|\mathbf{x}_1-\mathbf{x}_2|$. The zeroth-order diagram describes the contribution made by initial correlations among objects that have not captured any others. Since in the current approximation we have ignored the initial correlations, this diagram makes a trivial contribution:

$$P_0(r,R_1,R_2)=n_1n_2\theta(r-R_2)\{1+O(\epsilon)\},$$

$$n_1\equiv n(R_1),\quad n_2\equiv n(R_2).$$

The first diagram describes the contribution of binary systems:

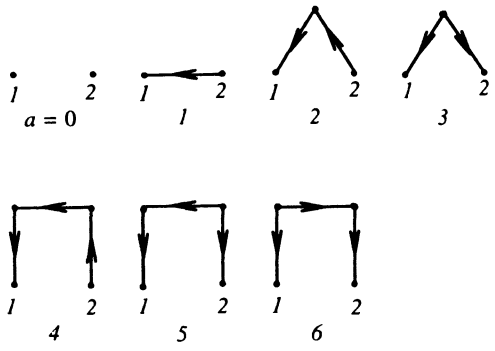

FIG. 4. Diagrams for $j=2$, $n\leqslant 4$, the leading diagrams in the small filling factor ϵ.

$$P_1(r,R_1,R_2)=n_1n_2\theta(R_2'-r)\left(\frac{3-\alpha}{3}\right)(1+z_2)^3\left(\frac{r}{R_2'}\right)^{-\alpha}, \tag{19}$$

where

$$z_2=R_2/R_2'-1=(R_2/R_2')^{3(n+3)/(n+5)}-1$$

[see (16)] is the redshift at the time corresponding to the larger member of the pair. When $r<R_2'$ and $R_1\neq R_2$, it is this diagram that provides the main contribution to the pairwise correlation function. The next two diagrams describe the contribution of ternary systems:

$$P_2(r,R_1,R_2)=n_1n_2\frac{2(3-\alpha)}{3(n+5)}A\left(\left(\frac{R_2'}{R_1'}\right)^{3-\alpha}-1\right)\times\beta(1+z_2)^3\left(\frac{r}{R_2'}\right)^{3-2\alpha},\quad r\ll R_2', \tag{20}$$

$$P_3(r,R_1,R_2)=n_1n_2\frac{(3-\alpha)}{16\gamma}A\left(\frac{17}{6}+\frac{22}{\gamma-6}\right)\times\beta(1+z_2)^3\left(\frac{r}{R_2'}\right)^{3-2\alpha},\quad r\ll R_2', \tag{21}$$

where $\gamma=(n+5)(3-\alpha)+3$, and A is a constant of order 1.

In (19), (20), and (21), we have written out the leading terms of the expansion in ϵ. It can be shown that the correlation function contains no other contributions that might diverge as $r\to 0$. Note that in calculating the dominant diagram of (17) we did not make use of the relation (15) between the formation time of an object and its size. If we were to do so, there would be no need to assume the validity of (15) when we considered the main contribution to the correlation function, and we could take R_i and z_i to be independent characteristics of the objects.

Furthermore, we can disregard assumption (18)—that the positions of the newly-formed objects are uncorrelated—and consider the case of arbitrary $P^n(\mathbf{y}_i,R_i)$. The contribution of the principal diagram then takes the form

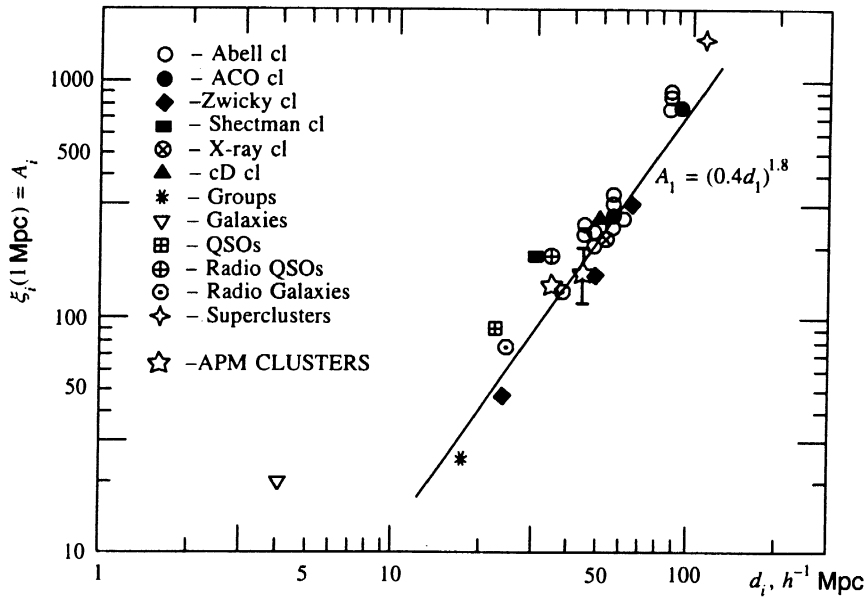

FIG. 5. Amplitude of the pairwise correlation function as a function of the mean distance between objects.[13]

$$P_1(r,R_1,R_2)=C(R_1,R_2)n_1n_2\theta(R_2'-r)\left(\frac{3-\alpha}{3}\right)\times(1+z_2)^3\left(\frac{r}{R_2'}\right)^{-\alpha},$$

where

$$C(R_1,R_2)=\frac{3}{4\pi n_1n_2R_2^3}\int_{|\mathbf{y}_1|<R_2}P^2(\mathbf{y}_1,\mathbf{0},R_1,R_2)d\mathbf{y}_1$$

does not depend on the r factor that takes initial correlations into account. Thus, the main contribution to the probability takes the form (23) even in the most general case, up to a factor C that does not depend on r.

In actuality, observable objects (such as clusters of a certain richness, etc.) cover a range of sizes from R_{i1} to R_{i2} (corresponding to a mass range of M_{i1} to M_{i2}), and possibly a range of formation times as well. A more accurate expression for the pairwise autocorrelation function, for example, would therefore be

$$\xi_i(r)=\frac{\int_{R_{i1}}^{R_{i2}}\int_{R_{i1}}^{R_{i2}}P(r,R_1,R_2)dR_1dR_2}{n_i^2}-1, \tag{22}$$

$$n_i=\int_{R_{i1}}^{R_{i2}}n(R)dR.$$

For the leading term in the strong-correlation range $\xi_i\gg 1$, (19) and (22) yield

$$\xi_i(r)=\left(\frac{ad_i}{r}\right)^{\alpha}, \tag{23}$$

where $d_i=n_i^{-1/3}$ is the mean separation between objects,

$$a=\beta^{1/3}\left(1-\frac{M_{i1}}{M_{i2}}\right)^{1/3}\left(\frac{3-\alpha}{3}\right)^{1/\alpha}(1+z_i)^{(3-\alpha)/\alpha}, \tag{24}$$

and

$$d_i=R_{i1}\beta^{-1/3}\left(1-\frac{M_{i1}}{M_{i2}}\right)^{-1/3}. \tag{25}$$

Here z_i is the mean time of formation of the objects considered, and $M_{i1,2}=(4/3)\pi\rho_0R_{i1,2}^3$. Note that the baryon-to-dark matter ratio is on average the same for the two objects, so the baryon masses M_{i1} and M_{i2} can be inserted in (24) and (25).

5. SUMMARY

We see, then, that binary systems make the major contribution to the pairwise correlation function in the strong-correlation range $\xi_i\gg 1$. Not only is that contribution the major one with regard to the parameter β, but it grows most rapidly with decreasing distance r. From (19), we see that the steady-state pairwise correlation of clusters, superclusters, etc. should grow as $r^{-\alpha}$ with decreasing distance, where $\alpha\approx 1.8$ is a universal scaling parameter that governs the three-dimensional nonlinear contraction of self-entrained nondissipative dark matter. This behavior is well known to be fully consistent with observed pairwise correlation functions of galaxies and clusters.[12] We therefore maintain that the theory of nonlinear contraction constructed in Refs. 1–3 has been confirmed by the observational data. Moreover, since substantial use was made in the derivation of Eq. (4) of the smallness of the thermal velocities of particles of dark matter, it would seem that the observations indirectly suggest that, to a large extent, dark matter is cold.

At high values of the correlation function, apart from the scaling law (23), its amplitude is observed to depend on the mean distance between objects. Figure 5 shows observational data taken from Ref. 13. In the distance range $20h^{-1}\mathrm{Mpc}<d_i<80h^{-1}\mathrm{Mpc}$, the observed amplitude A_i of the correlation function is

$$A_i=\xi_i(1\ \mathrm{Mpc})=(0.4d_i)^{1.8}. \tag{26}$$

As we showed above, objects of this size have yet to reach the end of the nonlinear stage of evolution (or have done so in the recent past), i.e., they were formed at a relatively small redshift and lie somewhere in the range $0<z_i<0.5$. The spread in z_i is then negligible, and the dependence of A_i on d_i given by theory [Eqs. (23) and (24)] is consistent with the observed dependence (26). It is clear from (26) and the figure that galaxies form—the amplitude of their correlation function is appreciably higher. The same effect is to be noted in quasars, albeit at a lesser level. Galaxies, however, come into being significantly earlier than the other objects plotted in Fig. 5. Assuming a mean redshift in (24) of $z_g \approx 5-7$ for galaxies and $z_q \approx 1.5-2$ for quasars, we obtain agreement with the observations. We note as well that the constant 0.4 in the experimental fitting function (26) is approximately twice the value obtained from Eqs. (23) and (24) for $z_i<0.5$.

Thus far, we have only discussed the main contribution to the correlation function in the range $\xi_i \gg 1$, which is, strictly speaking, the only range in which the equation derived above holds. This contribution comes solely from binary systems. The contribution to ξ_i from the next order in β depends on distance as $r^{3-2\alpha}$. It is small if the correlation function is calculated by averaging over a large enough region of space. It can become comparable to the contribution from the main term, however, if we consider, for example, only the immediate neighborhood of a large cluster of objects of a given type. As ξ decreases, the $r^{-\alpha}$ dependence will then change to $r^{3-2\alpha}$. Curiously enough, this sort of change in slope has been observed in the correlation function of galaxies in a cluster,[14] but a reliable comparison with the observations naturally requires further development of the theory discussed here. Specifically, to calculate ξ_i near 1, we need to take accurate account of initial correlations and the distribution of object formation times, and we need to specially examine the transition probability for objects that have not reached the steady state.

The authors are grateful to V. L. Ginzburg for his interest in this work. The participation of A. V. G. and K. P. Z. was supported by grant no. 93-02-17065 of the Russian Foundation for Fundamental Research. M. I. Z. was funded by the American Astronomical Society and the International Scientific Foundation's program of individual scientific grants.

[1] A. V. Gurevich and K. P. Zybin, Zh. Éksp. Teor. Fiz. **94**(1), 3 (1988) [Sov. Phys. JETP **67**, 1 (1988)].
[2] A. V. Gurevich and K. P. Zybin, Zh. Éksp. Teor. Fiz. **94**(10), 5 (1988) [Sov. Phys. JETP **67**, 1957 (1988)].
[3] A. V. Gurevich and K. P. Zybin, Zh. Éksp. Teor. Fiz. **97**, 20 (1990) [Sov. Phys. JETP **70**, 10 (1990)].
[4] M. Davis, G. Efstathiou, C. S. Frenk *et al.*, Astrophys. J. **292**, 371 (1985).
[5] J. P. Ostriker, Ann. Rev. Astron. Astrophys., ed. by G. Burbridge, D. Layzer, A. Sandage, Annual Review Inc., Palo Alto, CA **31**, 689 (1993).
[6] P. F. Smith and J. D. Lewin, Phys. Rep. **187**, 203 (1990).
[7] A. Linde, *Particle Physics and Inflationary Cosmology*, Nauka, Moscow (1990) [Harwood Academic Publishers, New York (1990)].
[8] E. M. Lifshitz, Zh. Éksp. Teor. Fiz. **16**, 587 (1946).
[9] N. A. Bahcall and R. Cen, Astrophys. J. **407**, L49 (1993).
[10] J. M. Bardeen, J. R. Bond, N. Kaiser, and A. S. Szalay, Astrophys. J. **304**, 15 (1986).
[11] P. J. E. Peebles, *The Large-Scale Structure of the Universe*, Princeton University Press, Princeton (1980).
[12] N. A. Bahcall and R. M. Soneira, Astrophys. J. **270**, 20 (1983).
[13] N. A. Bahcall and M. J. West, Astrophys. J. **392**, 419 (1992).
[14] M. Einasto, Mon. Not. R. Astron. Soc. **258**, 571 (1992).

Translated by Marc Damashek